POSS-bound ZnO nanowires as interphase for enhancing interfacial strength and hydrothermal aging resistance of PBO fiber/epoxy resin composites

Lei Chen[a,b], Zhen Hu[b], Zijian Wu[b], Guangshun Wu[b], Lichun Ma[b], Chunhua Zhang[b], Yudong Huang[*,b]

a College of Textiles and Garments, Southwest University, Chongqing 400715, PR China

b MIIT Key Laboratory of Critical Materials Technology for New Energy Conversion and Storage, School of Chemistry and Chemical Engineering, Harbin Institute of Technology, Harbin 150001, PR China

Abstract

A new hierarchical reinforcement was fabricated by growing ZnO nanowires (NWs) onto poly(*p*-phenylene benzobisoxazole) (PBO) fibers using a mild hydrothermal method, which served as a platform for the polyhedral oligomeric silsesquioxanes (POSS) grafting, using 3-aminopropyltrimethoxysilane (APTMS) as a bridging agent. Scanning electron microscopy (SEM) was employed to characterize the surface morphologies of PBO fibers and the de-bonding surface morphologies of their composites. Fourier transform infrared spectroscopy (FTIR) and X-ray photoelectron spectroscopy (XPS) confirmed the chemical bonding nature between ZnO NWs and APTMS, as well as between APTMS and POSS. The reinforcement offered a 83.4% enhancement in the interfacial shear strength (IFSS) without degrading the base fiber.

* Corresponding author. Tel/Fax: +86 451 86414806.
E-mail addresses: ydhuang.hit1@aliyun.com (Y.D. Huang).

Moreover, the possible interfacial property enhancing reasons were explored. The hydrothermal aging resistance of PBO/epoxy composite was also greatly improved.

Keywords: A. Fibres; A. Polymer-matrix composites (PMCs); B. Interface/interphase; D. Mechanical testing.

1. Introduction

Poly(*p*-phenylene benzobisoxazole) (PBO) fibers, representative of high-performance fibers, are widely used as reinforcements of advanced composites because of their excellent properties, such as high tensile strength, high thermal stability, light weight and relative flexibility [1-3]. Nevertheless, although the in-plane properties of their composites are excellent, the relatively poor interfacial properties remain a major challenge, which is due to their smooth and inert surfaces. To overcome the problem, a lot of researches have been devoted to the surface modification of PBO fibers [4-8].

In recent years, hierarchical composites composed of carbon nanotubes (CNTs) and high performance fibers have attracted wide attention, because CNTs work as lots of anchors to locally stiffen at the interfacial region and then accordingly improve the interfacial properties. The most common approach of growing CNTs onto fibers through chemical vapor deposition (CVD) processes carry out at a high temperature, which are less likely to be able to integrate with organic fibers [9, 10]. Recently, an alternative approach has been developed by Sodano's group to grow ZnO nanowires (NWs) onto carbon and aramid fibers from aqueous solutions at a low temperature

(<90 °C) [11-15]. Using this unique advantage of ZnO NWs growth, the interfacial shear strength (IFSS) of resulting composites is effectively enhanced. Meanwhile, the tensile strength (TS) testing shows the growth does not adversely affect fiber strength due to the mild reaction condition. However, it is noteworthy that the lack of chemical bonding between ZnO NWs and resin matrix limits the further increase of the interfacial properties of fiber composites [16].

Polyhedral oligomeric silsesquioxanes (POSS), a class of unique organic/inorganic components with a definite nanostructure, has become a new focus in material chemistry fields [17-19]. Having eight organic groups surrounding a cage-like core connected by Si-O-Si bonds, POSS is highly compatible in polymer matrix in comparison with other inorganic components, such as CNTs and ZnO NWs [20, 21]. Additionally, the organic groups can be used as reaction sites for further functionalization, making POSS an ideal modification reagent. During a thermal curing of composites, the temperature reached within the composite is high enough to create covalent bonding at the interface, delivering obviously improved interfacial properties [22, 23].

Chemically, the surface of ZnO NWs is mostly terminated by hydroxyl groups, which can be readily functionalized by various surface decorating molecules [24-26]. In this study, ZnO NWs are directly grown on the PBO fibers using a low-temperature hydrothermal growth strategy, mentioned in our previous work [16]. Then, the resulting ZnO NWs grown PBO fibers are functionalized with amine groups of

3-aminopropyltrimethoxysilane (APTMS), followed by grafting with octaglycidyldimethylsilyl POSS. The microstructure of obtained hierarchical reinforcement is systematically characterized. To substantiate the superior performance of the interfacial properties of PBO-ZnO-POSS/epoxy composite, a direct comparison is made with untreated PBO, PBO-COOH, PBO-ZnO NWs and PBO-ZnO-APTMS fibers. Furthermore, the hydrothermal aging resistance of their composites was investigated.

2. Experimental

2.1 Materials

The PBO fibers (Zylon, HM) with a filament diameter of 12 μm were supplied by Toyobo Ltd., Japan. Prior to use, surface sizing and contaminants of PBO fibers were removed by Soxhlet extraction with acetone at 70 °C for 48 h. Zinc acetate dihydrate [$Zn(CH_3COO)_2 \cdot 2H_2O$], zinc nitrate hexahydrate [$Zn(NO)_3 \cdot 6H_2O$], sodium hydroxide (NaOH), hexamethylenetetramine (HMTA), sulfuric acid (H_2SO_4), hydrochloric acid (HCl), chloroacetic acid, ethanol and tetrahydrofuran (THF) were purchased from Sinopharm Chemical Reagent Co., Ltd., China. 3-aminopropyltrimethoxysilane (APTMS) was received from TCI Ltd., Japan. Octaglycidyldimethylsilyl POSS (viscous liquid, cage content >65%, molecular weight 1337.88 and empiric formulae $C_{48}H_{88}O_{28}Si_8$) was purchased from Hybrid Plastics Co., Inc., USA. The molecular structure of POSS is demonstrated in Fig. 1. All chemicals and solvents were used as received.

2.2 Fabrication of PBO-ZnO-POSS

The PBO-ZnO-POSS hierarchical reinforcements were fabricated through several steps including fiber functionalization, ZnO NWs growth and modification processes, as illustrated in Fig. 2. As carboxyl groups have very strong chemical absorption with ZnO NWs [11], PBO fibers must be functionalized, which were borrowed from graphene oxide [27, 28]. PBO fibers were first etched in 60 wt% H_2SO_4 for 3 h. Afterwards the fibers were immersed in a solution containing 12 g NaOH and 100 mL deionized water. Then 10 g chloroacetic acid was added in the solution followed by ultrasonic for another 3 h to convert the hydroxyl groups to carboxyl groups via conjugation of acetic acid moieties giving PBO-COOH. The resulting fibers were rinsed with deionized water for several times and dried under vacuum.

To synthesize ZnO colloid suspension as quantum dot seeds, a 20 mM NaOH/ethanol solution and a 12.5 mM $Zn(CH_3COO)_2 \cdot 2H_2O$/ethanol solution were made by vigorously stirring at 50 °C for 10 min separately. Upon cooling, 40 mL NaOH/ethanol solution was then added into 320 mL ethanol, and 40 mL $Zn(CH_3COO)_2 \cdot 2H_2O$/ethanol solution was added into 100 mL ethanol. Then the two solutions were preheated separately to 65 °C and mixed for 30 min under vigorous stirring. The functionalized PBO fibers were dipped into the seed solution for 15 min, and then annealed at 150 °C for 10 min for a total of three times.

The ZnO NWs growth processes were as shown as follows, 3.125 mmol $Zn(NO)_3 \cdot 6H_2O$ and 3.125 mmol HMTA were dissolved in 500 mL deionized water, and the solution was heated with vigorous stirring until the temperature of water bath

reached 90 °C. The PBO fibers coated with ZnO seeds were immersed into the growth solution for 8 h, respectively. The resulting fibers, denoted as PBO-ZnO NWs, were rinsed with deionized water for several times and dried under vacuum.

The PBO-ZnO NWs were mixed with 0.5 g APTMS in 50 mL ethanol reacting at 40 °C for 24 h to obtain APTMS modified PBO fibers, denoted as PBO-ZnO-APTMS. 0.5 g POSS was dispersed in 50 mL THF under ultrasonic treatment for 30 min. Then the PBO-ZnO-APTMS were added in the above solution. After reaction at 50 °C for 12 h under nitrogen atmosphere, the resulting PBO fibers, denoted as PBO-ZnO-POSS, were rinsed with THF for several times and dried under vacuum.

2.3 Characterization of PBO fibers and their composites

Various PBO fibers were observed by a field emission scanning electron microscope (FE-SEM, JEOL JSM-6335F, Japan) and a transmission scanning electron microscope (TEM, Hitachi H-7650, Japan). Fourier-transform infrared spectrometer (FTIR, Nicolet Nexus670, USA) and X-ray photoelectron spectroscopy (XPS, Thermo Scientific, USA) were employed to measure the surface chemical composition of PBO fibers.

The surface wettability of PBO fibers was tested by measuring the increasing weight when they were dipped into the epoxy resin. At first the value was recorded with intervals of 1 s, then 3 s, at last 30 s.

Monofilament tensile tests were conducted on a universal testing machine (Instron 5566, USA) according to ASTM D3379-75. The gauge length was 100 mm, and the

cross-head speed was 10 mm/min. The tensile strength (TS) results were analyzed by a Weibull statistical method.

Monofilament pull-out tests were performed to determine the interfacial shear strength (IFSS) of PBO/epoxy composites using an interfacial strength evaluation equipment (Tohei Sanyon Co Ltd, Japan). A PBO monofilament was fastened to a metal holder with dimension of 70 mm × 35 mm. Some epoxy droplets were placed against the monofilament with the embedded length of 100-140 μm using a fine-point tip applicator. The specimens were cured at 90 °C for 2 h, then at 120 °C for 2 h and finally at 150 °C for 3 h. After curing treatment, an epoxy droplet was blocked and loaded by two metal blades at a cross-head speed of 0.06 mm/min. The values of IFSS were calculated from Eq. (1).

$$\mathrm{IFSS} = \frac{F_{\max}}{\pi d l} \tag{1}$$

where $F_{\max}$ is the peak pullout force; d is the monofilament diameter; and l is the embedded length of monofilament in epoxy resin.

The PBO/epoxy composites were immersed in boiling water for 24 h and 48 h, respectively. Afterwards the hydrothermal aging resistance was assessed by tracing the changes in their IFSS results.

3. Results and discussion

Fig. 3 shows the surface morphologies of PBO fibers before and after modification. Compared to the smooth surface of untreated-PBO (Fig. 3a), there are some narrow grooves distributing along the axial direction of PBO-COOH, as shown in Fig. 3b. After

the growth of ZnO NWs (Fig. 3c and d), striking differences in the surface morphology can be clearly observed. The fiber surface is covered by dense arrays of "needle-like" ZnO NWs. PBO fiber grown with highly uniform and vertically oriented of ZnO NWs are successfully achieved. The APTMS-modified ZnO NWs retain a smooth surface similar to that of pristine ZnO NWs (Fig. 3e and f), which agrees well with the previous result [29]. In the case of PBO-ZnO-POSS (Fig. 3g and h), the surface of ZnO NWs becomes rougher, providing direct evidence for the grafting of POSS. Some ZnO NWs detach from the fiber surface after two reaction steps. Thus, the density of POSS modified ZnO NWs is lower than the pristine ZnO NWs. From Fig. 4, the POSS modified ZnO NWs bridging PBO fiber and resin matrix are observed, suggesting high surface wettability and reactivity with the matrix.

Fig. 5 diplays the FTIR spectra of different PBO fibers. All five specimens present the characteristic bands of PBO, a C=N stretching at 1636 cm^{-1}, a C–O–C stretching at 1054 cm^{-1} and an aromatic C–H stretching at 3000 cm^{-1} [30]. For the PBO-COOH, a new characteristic band appears at 1726 cm^{-1} which is assigned to the stretching vibration of carboxyl groups, indicating that the PBO fiber has been functionalized successfully. After the growth of ZnO NWs, PBO fibers exhibit the absorption bands at 470 cm^{-1} and 3444 cm^{-1} originated from the Zn–O and O–H stretching, respectively [25]. Upon modified with APTMS, the O–H band is shifted to 3510 cm^{-1}, originating from the N–H stretching. In the case of PBO-ZnO-POSS, the band at 1694 cm^{-1} is assigned to the C=O stretching of amide (amide I band), and the band at 1554 cm^{-1} corresponds to

the N–H scissoring of amide (amide II band). The strong band centered at 1055 cm^{-1} corresponds to Si–O–Si stretching vibration. The FTIR results prove the POSS is grafted onto the fiber surface through covalent bonds.

Wide-scan survey XPS spectra are used to further examine the chemical compositions of PBO fiber surface, as shown in Fig. 6a. We can find that both untreated-PBO and PBO-COOH surfaces are composed of carbon, oxygen and nitrogen elements. In the PBO-COOH spectrum, the carbon content decreases, while the oxygen content increases sharply. Some of the carbon atoms on the fiber surface are converted to the carboxyl groups, which form strong interaction with ZnO NWs [11]. After the growth of ZnO NWs, XPS signals from Zn are detected, indicating a successful growth of ZnO NWs onto the fiber surface. After being modified with APTMS and POSS (Fig. 6b), Si2p peaks appear at 104.1 eV. Compared to PBO-ZnO-APTMS, the silica content of PBO-ZnO-POSS increases form 9.81% to 12.23%, which is caused by the grafting of Si–O cores of POSS on the fiber surface. To confirm the APTMS and POSS modification of ZnO NWs, N1s peaks of XPS spectra are shown in Fig. 6c-g. The N1s peak positions derive from peak deconvolution results. For untreated-PBO, PBO-COOH and PBO-ZnO NWs fibers (Fig. 6c-e), only one –N= peak at 399 eV is observed. After being modified with APTMS (Fig. 6f), the XPS result shows a new peak at 400 eV, attributable to N–H species, respectively. The $–NH_2$ species is assigned to APTMS, which confirms the presence of APTMS on the fiber surface [7]. In the case of PBO-ZnO-POSS (Fig. 6g), an additional peak at 401.7 eV ascribes to N–C=O appears,

indicating the occurrence of a chemical reaction between the amine groups of APTMS and the epoxy groups of POSS.

The mechanical properties of PBO fibers and their composites are evaluated by ~~TS~~ tensile (Fig. 7a) and ~~IFSS~~ interfacial (Fig. 7b) tests. The TS values of untreated-PBO fiber, PBO-COOH, PBO-ZnO NWs, PBO-ZnO-APTMS and PBO-ZnO-POSS are 5.8, 5.51, 5.53, 5.32 and 5.15 GPa, respectively. We can also directly observe the changes of tensile strength, elongation at break and Youngs' modulus before and after modification through their typical stress-strain curves, as depicted in Fig. S1. Obviously, the multi-step processes do not cause any discernable decrease in the ~~TS~~ mechanical properties of PBO fibers. After fiber functionalization, the IFSS of PBO/epoxy composite increases from 40.4 to 52.2 MPa. Upon being grown with ZnO NWs, the IFSS increases to 60.9 MPa, which is mainly attributed to the increased bonding area and mechanical interlocking. After being modified with APTMS, the IFSS shows a increase to 65.2 MPa. By contrast, the PBO-ZnO-POSS/epoxy composite has the highest IFSS value (74.1 MPa), which gives rise to a 83.4% enhancement compared to untreated-PBO/epoxy composite, and a 13.5% enhancement compared to PBO-ZnO-APTMS/epoxy composite. The epoxy groups on the POSS side chains play an important role in improving the interfacial adhesion between the fiber and the matrix. These polar groups can increase the surface energy of PBO fibers, and make the fiber surface easier to be wetted by resin matrix. Moreover, the epoxy groups on the fiber surface can react with the curing agent in the resin system, which can form a strong

covalent bond at the interfacial region.

It is noteworthy that many methods have been used to enhance the interfacial adhesion between PBO fibers and resin matrix. Li et al. reported that the IFSS of composite was remarkably increased from 35.8 to 60.3 MPa by grafting GO onto PBO fibers via a solvothermal method [31]. Gu et al. proposed a "three-step approach" of methanesulfonic acid/γ-aminopropyl triethoxy silane/glycidylethyl polyhedral oligomeric silsesquioxane (MSA/KH550/POSS) to modify the surface of PBO fibers, and found that the IFSS of PBO/epoxy composite was increased by 26.6% [32]. Compared to the previous reports, the surface modification method combining whiskerization and chemical grafting also shows promising results for interface improvement.

The overall performance of fiber reinforced polymer composites is closely related to the surface wettability of reinforcement with matrix. The increase of the surface free energy leads to better wettability between PBO fiber and matrix, and improvement of the interface adhesion [16]. Dynamic wetting curves of different PBO fibers in epoxy resin are presented in Fig. 7c. The absorption weights of untreated-PBO and PBO-COOH are 0.135 and 0.147 $g \cdot g^{-1}$, respectively. After the growth of ZnO NWs, the adsorption weight increases to 0.176 $g \cdot g^{-1}$, attributable to the increased contact area and Van der Waals interactions. After being modified with APTMS and POSS, the absorption weight increases remarkably to 0.198 and 0.218 $g \cdot g^{-1}$, respectively. The significantly improved wettability between the fiber and the matrix is ascribed to the

enhanced surface free energy and the introduced polar groups. These polar amine and epoxy groups on the PBO fiber surface have an excellent wettability and adsorption with the epoxy matrix to maximize the molecular contact degree at the interfacial region. The sufficient contact at a molecular level not only reduces defects, voids or cracks in the interfacial region, but also forms much stronger chemical bonding and mechanical interlocking, which are beneficial to the interfacial adhesion and overall properties of resulting composites.

To further identify the reasons for the improvement of interfacial properties of composites, the de-bonding surface morphologies of PBO/epoxy composites are also examined. Fig. 7d shows the epoxy droplet image before de-bonding. Obviously, the epoxy droplet was completely intact. The surface morphologies of PBO fibers de-bonded from the matrix are given in Fig. 7e and f. There are few epoxy fragments remaining on the de-bonded surface of untreated-PBO (Fig. 7e), showing easily de-bonding due to the weak van der Waals force between the fiber and the matrix. The appearance of gap at interfacial region (marked by frame) also indicates poor interfacial properties of untreated-PBO/epoxy composite. In the case of PBO-ZnO-POSS (Fig. 7f), many epoxy fragments are observed on the de-bonded surface of the fiber, and no gap is found between the fiber and the matrix, indicating a stronger mechanical interlocking. Our group has successfully grown ZnO NWs on PBO fibers through a hydrothermal method, and then investigated the IFSS of PBO/epoxy composite [16]. Although the ZnO NWs as interphase enhance the interfacial properties of the resulting composites by

increasing mechanical interlocking, poor surface wettability limits its further improvement of the overall performance of composite. In this study, POSS modified ZnO NWs improve not only the surface wettability but also the reactivity with the matrix. As a result, the polar epoxy resin can easily wet the surface of PBO fibers, resulting in a strong interface. Without doubt, the growth of ZnO NWs can form two interfaces one between the PBO fiber and ZnO and a second between the ZnO and resin matrix, and we can imply from Fig. S2 that the failure at the ZnO/PBO fiber interface is the major mode, which is analogous to the CNTs fracture during carbon fiber de-bonding observed by Hung [33]. Some ZnO NWs attached with epoxy fragments can be traced on the fiber surface (marked by frame), indicating a stronger mechanical interlocking between fiber and resin matrix.

High humidity may destroy the interface of PBO/epoxy composites, and deteriorate their mechanical properties. Therefore, the effects of hydrothermal aging time on the interfacial properties of PBO/epoxy composites are evaluated, as shown in Fig. 8. The IFSS of untreated-PBO/epoxy composite declines quickly during the hydrothermal aging process, whereas the IFSS of PBO-ZnO-POSS/epoxy composite decreases much slower. After 48 h hydrothermal aging, the IFSS retention ratios of untreated-PBO/epoxy and PBO-ZnO-POSS/epoxy composites are 59.3% and 71.7%, respectively. Clearly, the IFSS retention ratio of PBO-ZnO-POSS/epoxy composite is much higher than that of untreated-PBO/epoxy composite, implying an outstanding hydrothermal aging resistance. Many microcracks are formed in the hydrothermal

environment due to a great difference of coefficient of thermal expansion between PBO fiber and epoxy resin. Water molecules can penetrate through these microcracks into the interfacial region of the composites, resulting in the damage of the interface. The ZnO NWs acting as a buffer layer may reduce the number of microcracks. Moreover, the N–C=O bonds have formed at the interface of the PBO-ZnO-POSS/epoxy composite, which hydrolysis needs strong base over a long period of time [34]. Therefore, PBO-ZnO-POSS/epoxy composite displays better hydrothermal aging resistance than that of untreated one.

4. Conclusions

In summary, a new hierarchical reinforcement was fabricated by grafting POSS onto ZnO NWs grown PBO fibers using APTMS as the coupling agent. The IFSS of PBO/epoxy composite was dramatically enhanced by 83.4%. The increased surface wettability and reactivity with the matrix were the main contributors for such an enhancement. Meanwhile, the modification processes did not lead to any discernable decrease in TS. Furthermore, the N–C=O bonds at the interface of composite effectively improved the hydrothermal aging resistance.

Acknowledgements

We gratefully acknowledge financial support by the Chang Jiang Scholars Program and National Science Foundation of China (no. 51273050).

Supplementary material

Typical stress-strain curves of different PBO fibers; Cross-sectional SEM image of

PBO-ZnO-POSS/epoxy composite.

References

[1] Ran S, Burger C, Fang D, Zong X, Chu B, Hsiao BS, et al. A synchrotron WAXD study on the early sages of coagulation during PBO fiber spinning. Macromolecules 2002;35(27):9851-3.

[2] Hu Z, Li J, Tang PY, Li DL, Song YJ, Li YW, et al. One-pot preparation and continuous spinning of carbon nanotube/poly(*p*-phenylene benzobisoxazole) copolymer fibers. J Mater Chem 2012;22(37):19863-71.

[3] Hu Z, Li N, Li J, Zhang C, Song Y, Li X, et al. Facile preparation of poly(p-phenylene benzobisoxazole)/graphene composite films via one-pot in situ polymerization. Polymer 2015;71:8-14.

[4] Wu GM, Shyng YT. Surface modification and interfacial adhesion of rigid rod PBO fibre by methanesulfonic acid treatment. Composites Part A 2004;35(11):1291-300.

[5] Liu D, Hu J, Zhao Y, Zhou X, Ning P, Wang Y. Surface modification of PBO fibers by argon plasma and argon plasma combined with coupling agents. J Appl Polym Sci 2006;102(2):1428-35.

[6] Qian J, Wu J, Liu X, Zhuang Q, Han Z. Improvement of interfacial shear strengths of polybenzobisoxazole fiber/epoxy resin composite by n-TiO_2 coating. J Appl Polym Sci 2013;127(4):2990-5.

[7] Chen L, Wei F, Liu L, Cheng WL, Hu Z, Wu GS, et al. Grafting of silane and graphene oxide onto PBO fibers: Multifunctional interphase for fiber/polymer matrix

composites with simultaneously improved interfacial and atomic oxygen resistant properties. Compos Sci Technol 2015;106:32-38.

[8] Chen L, Du Y, Huang Y, Wu F, Cheng HM, Fei B, et al. Hierarchical poly(*p*-phenylene benzobisoxazole)/graphene oxide reinforcement with multifunctional and biomimic middle layer. Composites Part A 2016;88:123-30.

[9] Sager RJ, Klein PJ, Lagoudas DC, Zhang Q, Liu J, Dai L, et al. Effect of carbon nanotubes on the interfacial shear strength of T650 carbon fiber in an epoxy matrix. Compos Sci Technol 2009;69(7-8):898-904.

[10] Zhang Q, Liu J, Sager R, Dai L, Baur J. Hierarchical composites of carbon nanotubes on carbon fiber: Influence of growth condition on fiber tensile properties. Compos Sci Technol 2009;69(5):594-601.

[11] Lin Y, Ehlert G, Sodano HA. Increased interface strength in carbon fiber composites through a ZnO nanowire interphase. Adv Funct Mater 2009;19(16):2654-60.

[12] Ehlert GJ, Sodano HA. Zinc oxide nanowire interphase for enhanced interfacial strength in lightweight polymer fiber composites. ACS Appl Mater Iterfaces 2009;1(8):1827-33.

[13] Galan U, Lin Y, Ehlert GJ, Sodano HA. Effect of ZnO nanowire morphology on the interfacial strength of nanowire coated carbon fibers. Compos Sci Technol 2011;71(7):946-54.

[14] Ehlert GJ, Galan U, Sodano HA. Role of surface chemistry in adhesion between ZnO nanowires and carbon fibers in hybrid composites. ACS Appl Mater Iterfaces

2013;5(3):635-45.

[15] Hwang H-S, Malakooti MH, Sodano HA. Tailored interyarn friction in aramid fabrics through morphology control of surface grown ZnO nanowires. Composites Part A 2015;76:326-33.

[16] Chen L, Liu L, Du YZ, Cheng WL, Hu Z, Wu GS, et al. Processing and characterization of ZnO nanowire-grown PBO fibers with simultaneously enhanced interfacial and atomic oxygen resistance properties. RSC Adv 2014;4(104):59869-76.

[17] Leu C-M, Chang Y-T, Wei K-H. Polyimide-side-chain tethered polyhedral oligomeric silsesquioxane nanocomposites for low-dielectric film applications. Chem Mater 2003;15(19):3721-7.

[18] Liu H, Zheng S, Nie K. Morphology and thermomechanical properties of organic-inorganic hybrid composites involving epoxy resin and an incompletely condensed polyhedral oligomeric silsesquioxane. Macromolecules 2005;38(12):5088-97.

[19] Valentini L, Bon SB, Monticelli O, Kenny JM. Deposition of amino-functionalized polyhedral oligomeric silsesquioxanes on graphene oxide sheets immobilized onto an amino-silane modified silicon surface. J Mater Chem 2012;22(13):6213-7.

[20] Atar N, Grossman E, Gouzman I, Bolker A, Murray VJ, Marshall BC, et al. Atomic-oxygen-durable and electrically-conductive CNT-POSS-polyimide flexible films for space applications. ACS Appl Mater Interfaces 2015;7(22):12047-56.

[21] Cardiano P, Fazio E, Lazzara G, Manickam S, Milioto S, Neri F, et al. Highly

untangled multiwalled carbon nanotube@polyhedral oligomeric silsesquioxane ionic hybrids: Synthesis, characterization and nonlinear optical properties. Carbon 2015;86:325-37.

[22] Zhao F, Huang Y. Preparation and properties of polyhedral oligomeric silsesquioxane and carbon nanotube grafted carbon fiber hierarchical reinforcing structure. J Mater Chem 2011;21(9):2867-70.

[23] Zhao F, Huang YD, Liu L, Bai YP, Xu LW. Formation of a carbon fiber/polyhedral oligomeric silsesquioxane/carbon nanotube hybrid reinforcement and its effect on the interfacial properties of carbon fiber/epoxy composites. Carbon 2011;49(8):2624-32.

[24] Kim JY, Osterloh FE. ZnO-CdSe nanoparticle clusters as directional photoemitters with tunable wavelength. J Am Chem Soc 2005;127(29):10152-3.

[25] Lee J, Choi S, Bae SJ, Yoon SM, Choi JS, Yoon M. Visible light-sensitive APTES-bound ZnO nanowire toward a potent nanoinjector sensing biomolecules in a living cell. Nanoscale 2013;5(21):10275-82.

[26] Jiang X, Wang H, Yuan R, Chai Y. Sensitive electrochemiluminescence detection for CA15-3 based on immobilizing luminol on dendrimer functionalized ZnO nanorods. Biosens Bioelectron 2015;63:33-8.

[27] Sun X, Liu Z, Welsher K, Robinson JT, Goodwin A, Zaric S, et al. Nano-graphene oxide for cellular imaging and drug delivery. Nano Res 2008;1(3):203-12.

[28] Hu Z, Li J, Li C, Zhao S, Li N, Wang Y, et al. Folic acid-conjugated graphene–ZnO nanohybrid for targeting photodynamic therapy under visible light irradiation. J Mater

Chem B 2013;1(38):5003-13.

[29] Guo CX, Dong Y, Yang HB, Li CM. Graphene quantum dots as a green sensitizer to functionalize ZnO nanowire arrays on F-doped SnO_2 glass for enhanced photoelectrochemical water splitting. Adv Energy Mater 2013;3(8):997-1003.

[30] Li Y, Li J, Song Y, Hu Z, Zhao F, Huang Y. *In situ* polymerization and characterization of graphene oxide-co-poly(phenylene benzobisoxazole) copolymer fibers derived from composite inner salts. J Polym Sci Part A 2013;51(8):1831-42.

[31] Li YW, Zhao F, Song YJ, Li J, Hu Z, Huang YD. Interfacial microstructure and properties of poly(phenylene benzobisoxazole) fiber grafted with graphene oxide via solvothermal method. Appl Surf Sci 2013;266:306-12.

[32] Gu J, Bai T, Dang J, Feng J, Zhang Q. Surface functionalization of HMPBO fibers with MSA/KH550/GlycidylEthyl POSS and improved interfacial adhesion. Polym Compos 2014;35(3):611-6.

[33] Hung KH, Kuo WS, Ko TH, Tzeng SS, C.F. Yan. Processing and tensile characterization of composites composed of carbon nanotube. Composites Part A 2009;40(8):1299-304.

[34] Cao K, Siepermann CP, Yang M, Waas AM, Kotov NA, Thouless MD, et al. Reactive aramid nanostructures as high-performance polymeric building blocks for advanced composites. Adv Funct Mater 2013;23(16):2072-80.

Figure captions

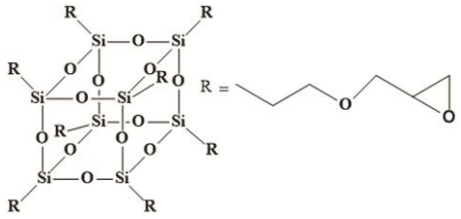

Fig. 1. Molecular structure of POSS.

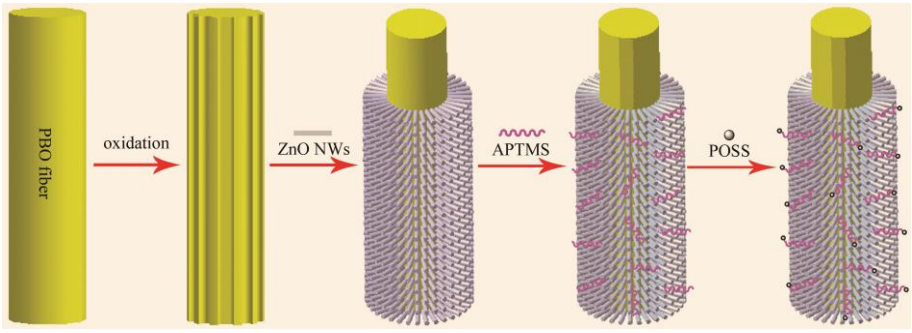

Fig. 2. Schematic of the fabrication procedure of PBO-ZnO-POSS.

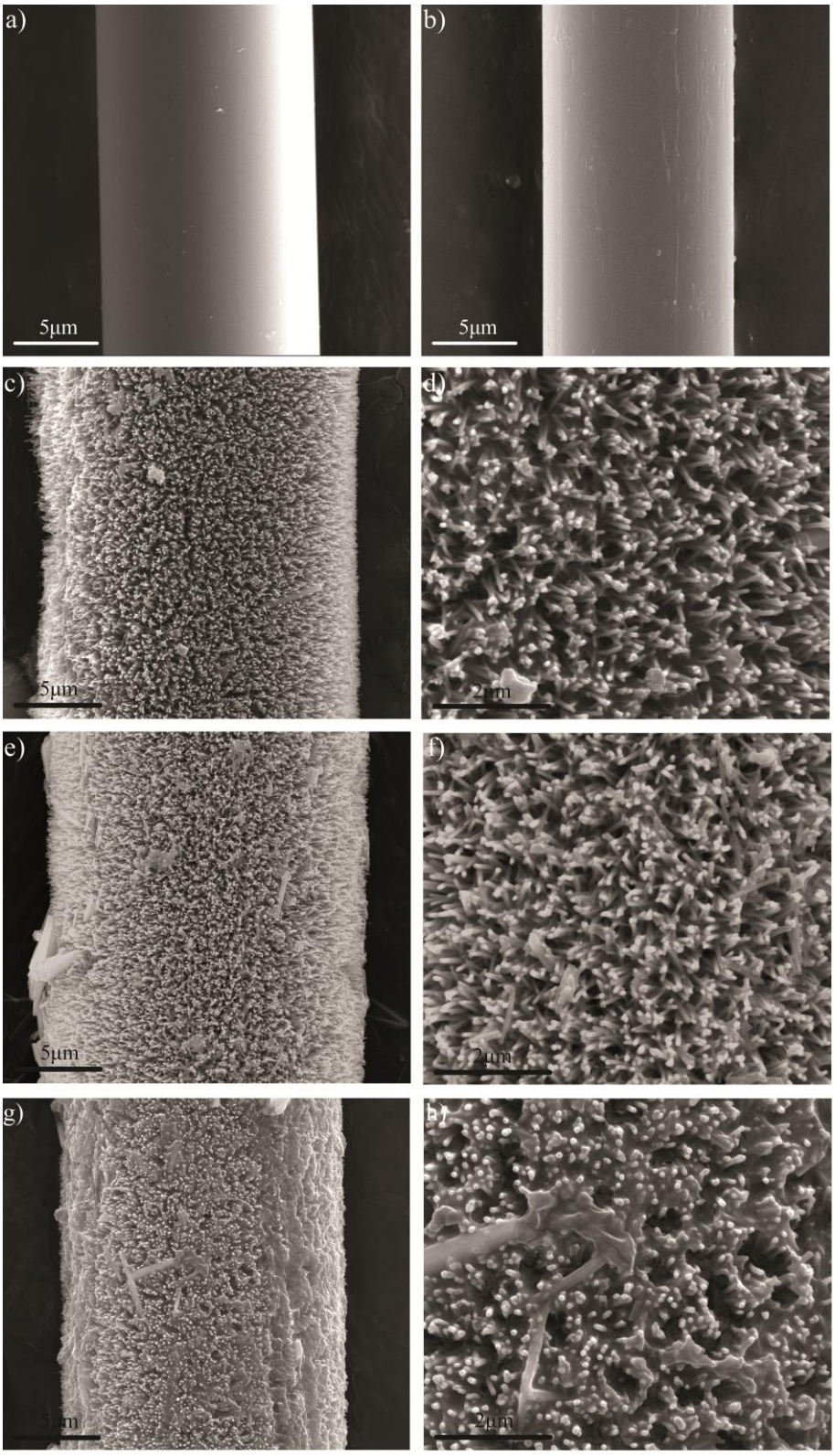

Fig. 3. SEM images of a) untreated-PBO; b) PBO-COOH; c), d) PBO-ZnO NWs; e), f) PBO-ZnO-APTMS and g), h) PBO-ZnO-POSS.

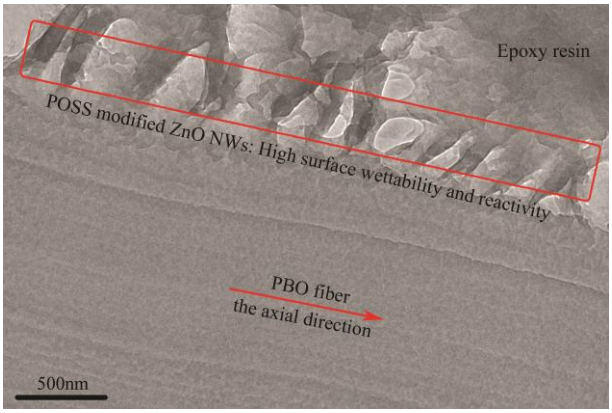

Fig. 4. Cross-sectional TEM image of PBO-ZnO-POSS.

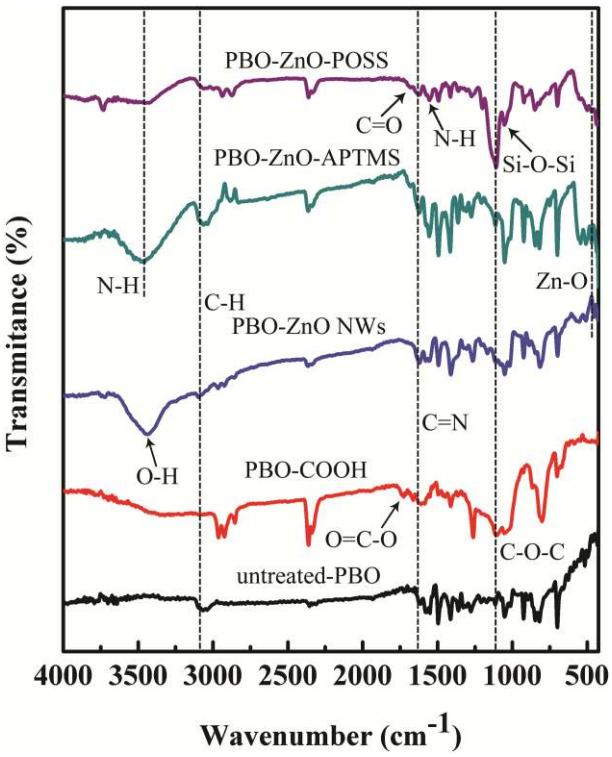

Fig. 5. FTIR spectra of different PBO fibers.

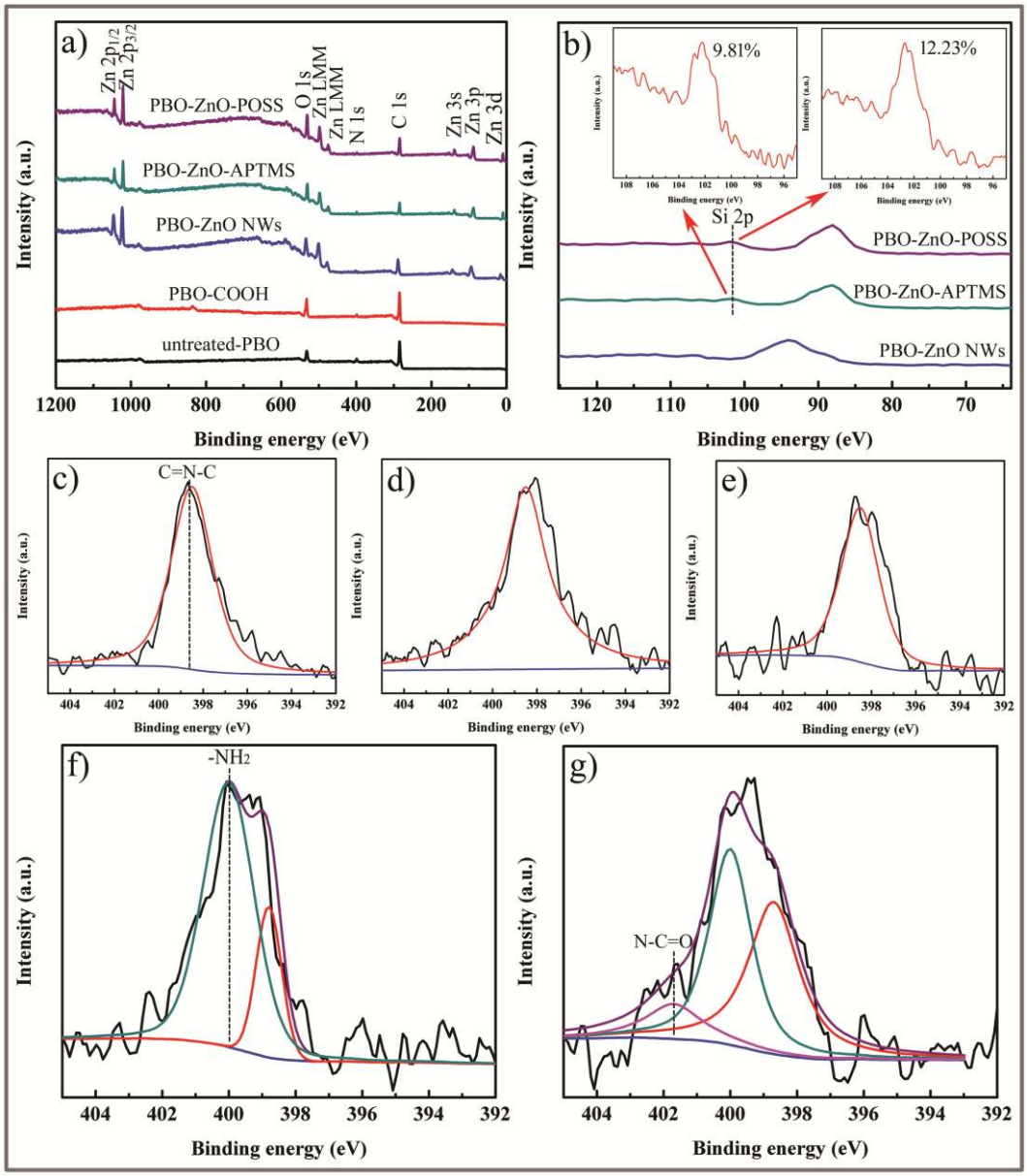

Fig. 6. a), b) Wide-scan survey XPS spectra of PBO fibers; XPS N1s spectra and fitted curves of c) untreated-PBO, d) PBO-COOH, e) PBO-ZnO NWs, f) PBO-ZnO-APTMS and g) PBO-ZnO-POSS.

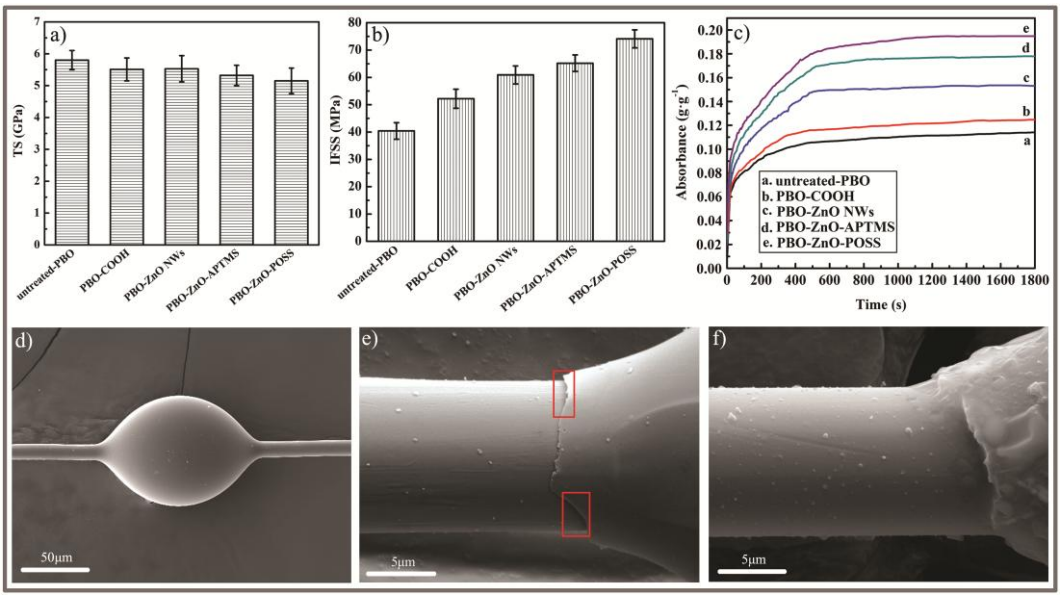

Fig. 7. a) TS of different PBO fibers; b) IFSS of different PBO/epoxy composites; c) dynamic wetting curves of different PBO fibers; SEM images of d) an epoxy droplet before de-bonding, e) untreated-PBO and f) PBO-ZnO-POSS composites after de-bonding.

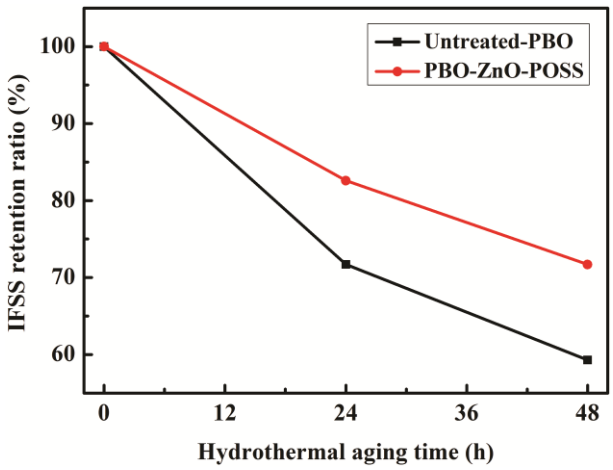

Fig. 8. IFSS retention of different PBO/epoxy composites after hydrothermal aging.